

Valence Instability in $\text{Eu}(\text{Pd}_{1-x}\text{Au}_x)_2\text{Si}_2$: The Global Phase Diagram

C. U. Segre, M. Croft, and J. A. Hodges

Department of Physics, Rutgers, The State University, Piscataway, New Jersey 08854

and

V. Murgai, L. C. Gupta, and R. D. Parks

Department of Physics, Polytechnic Institute of New York, Brooklyn, New York 11201

(Received 13 October 1982)

A system has been discovered in which the characteristic energies of a valence instability and a magnetic ordering instability can be brought into parity. This leads to a novel phase diagram where a line of second-order magnetic transitions terminates at a line of first-order valence transitions which, in turn, terminates at a critical point. Microscopic Mössbauer-effect measurements of the order parameters across both magnetic and valence instabilities, along with bulk magnetic susceptibility measurements, are presented.

PACS numbers: 64.70.Kb, 75.30.Kz, 76.80.+y

Although many Ce, Sm, Eu, and Yb compounds exhibit valence and coupled magnetic-nonmagnetic instabilities, no general phase diagrams of these systems have yet been determined.¹⁻⁴ Here we present the comprehensive phase diagram (including both magnetic and valence transitions) for an Eu compound subject to a valence instability (Fig. 1). This phase diagram can serve as a "blueprint" for the physics underlying the crossover between the highly magnetic, $J = \frac{7}{2}$, Eu^{2+} state and the nonmagnetic, $J = 0$, Eu^{3+} state. Global phase diagrams have previously played key roles in the studies of metal-insulator transitions in electron-hole droplets⁵ and in transition-metal compounds.⁶

Compounds with composition $\text{Eu}(\text{Pd}_{1-x}\text{Au}_x)_2\text{Si}_2$, $0 \leq x \leq 1$, crystallize in the tetragonal ThCr_2Si_2 structure.⁷⁻⁹ Magnetic susceptibility, x-ray diffraction, and Mössbauer-effect measurements indicate that EuPd_2Si_2 undergoes a precipitous, yet

continuous, valence change centered about 140 K.⁷⁻¹⁰ Extensive Mössbauer-effect studies have established that strong intersite interaction effects sharpen the thermal valence variation of EuPd_2Si_2 to the verge of a first-order valence transition.¹⁰ At present it is unclear whether the microscopic driving mechanism for these intersite interactions is dominantly electronic or elastic.

Through determination of the ¹⁵¹Eu isomer shift, Mössbauer-effect experiments yield a direct measurement of the Eu valence state.¹¹ If I_2 and I_3 are, respectively, the isomer shifts of ¹⁵¹Eu²⁺ and ¹⁵¹Eu³⁺ in a given crystal environment, then the average isomer shift is given by $\bar{I} = I_2 P_2 + I_3 P_3$ where P_2 (P_3) is the occupation probability of the 2+ (3+) valence state.¹¹ In order to obtain an estimate of nominal valence from the isomer-shift data of $\text{Eu}(\text{Pd}_{1-x}\text{Au}_x)_2\text{Si}_2$ compounds, $I_3 = -0.5$ mm/s and $I_2 = -11$ mm/s were used. These values were chosen close to the isomer shifts of 3+ EuFe_2Si_2 (-0.7 mm/s) and 2+ EuAg_2Si_2 (-11.4 mm/s), compounds which also crystallize in the ThCr_2Si_2 structure.¹² All isomer shifts are quoted relative to a Sm_2O_3 source. It should be emphasized that the valence estimates are only approximate because of the intrinsic uncertainty in I_2 and I_3 .

The phase diagram for the valence instability of the $\text{Eu}(\text{Pd}_{1-x}\text{Au}_x)_2\text{Si}_2$ system (Fig. 1) has five main features: (1) a line of continuous valence transitions (dashed line); (2) a critical point separating continuous and first-order valence transitions (solid circle); (3) a line of first-order valence transitions (heavy solid line); (4) a shaded

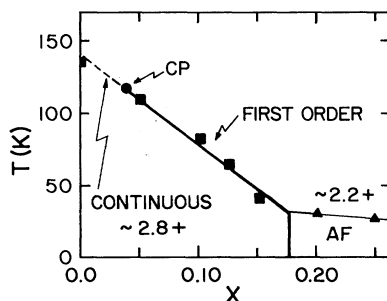


FIG. 1. Phase diagram for the $\text{Eu}(\text{Pd}_{1-x}\text{Au}_x)_2\text{Si}_2$ systems, discussed in the text. The shaded region indicates the inhomogeneity smearing of the valence transition in this and subsequent figures.

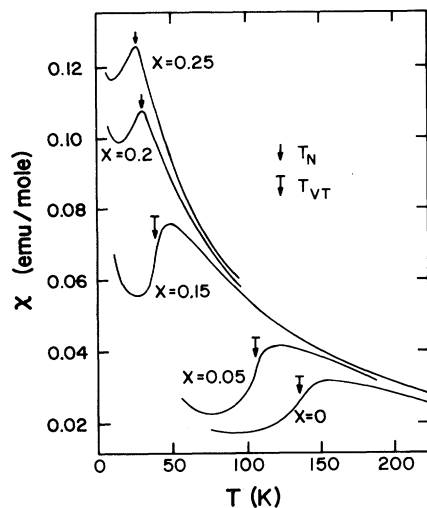


FIG. 2. Magnetic susceptibility vs temperature for selected samples in the $\text{Eu}(\text{Pd}_{1-x}\text{Au}_x)_2\text{Si}_2$ system. The arrows (\downarrow) indicate Néel temperatures (T_N) and the crossbarred arrows ($\bar{\downarrow}$) indicate valence transition temperatures (T_{VT}). The upturns at low temperatures are most likely due to untransformed Eu^{2+} as suggested by high-field magnetization experiments (Ref. 9).

region indicating roughly the 25%–75% completion of the inhomogeneity-smearred first-order valence transition; and (5) a line of antiferromagnetic transitions (light solid line). The experimental valence transition temperatures (squares) and antiferromagnetic transitions (triangles) were determined by a combination of Mössbauer-effect and magnetic susceptibility (χ) measurements.

The valence transition temperatures for all alloys were defined as the temperature where $d\chi/dT$ showed a pronounced peak [i.e., where $\chi(T)$ showed the greatest slope, Fig. 2]. This is in

analogy to previous results on the γ - α transition in Ce-based systems.¹³ In the case of continuously transforming samples (x close to 0) this temperature coincided, within experimental error, with the inflection point of the isomer shift versus temperature data [see the data for EuPd_2Si_2 in Fig. 3(a)]. In samples which showed a first-order valence transition, the Mössbauer-effect results indicated a smearing of the transition over a finite temperature range. Low-temperature x-ray diffraction results have shown that this smearing of the valence transition is due to spatially distinct regions transforming at different temperatures.¹⁴ One potential cause for the observed spatial inhomogeneity is variations in internal pressure due to the anisotropic contraction of crystallites. The presence of such internal stresses is clear from electrical resistivity measurements which reveal thermal-cycling-induced cracking of the samples.^{9,15} A second potential source of spatial inhomogeneities is through Au-Pd composition fluctuations. The temperature where the transition was $\sim 50\%$ complete as determined by the Mössbauer effect coincided with the transition temperature as defined by the peak in $d\chi/dT$.

The data on isomer shift versus temperature for an $x = 0.15$ sample [Fig. 3(a)] show a first-order valence transition. Mössbauer spectra in the first-order transition region were bimodal. Careful fitting of the spectra in this region showed a systematic transfer of intensity from an ~ 2.2 -valent absorption line to an ~ 2.8 -valent line with decreasing temperature. The shaded area in Fig. 2 (as in Fig. 1) indicates the 75%–25% completion limits of the smeared first-order transition. Details of this fitting procedure and a dis-

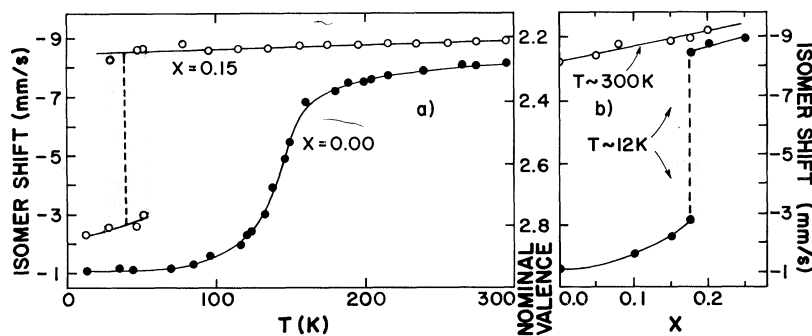


FIG. 3. (a) Thermal variation of the isomer shifts for an $x = 0.15$ sample (and for an $x = 0.00$ sample for comparison). The open circles are the isomer shifts of the $\text{Eu}^{2,2+}$ and $\text{Eu}^{2,8+}$ lines in the $x = 0.15$ sample. The solid lines are guides to the eye, the dashed line indicates the valence transition temperature assigned as described in the text. (b) Isomer-shift variation as a function of x across the valence transition at $T \sim 12\text{K}$ and at $T \sim 300\text{K}$ where no valence transition occurs.

discussion of residual absorption intensity centered between the two main lines is discussed elsewhere.¹⁶

When the isomer shift is plotted versus x for $T = 300$ K and $T \sim 10$ K [Fig. 3(b)], a first-order valence transition is again visible. At $T = 300$ K the isomer shift (valence) variation is monotonic in x , since the valence instability line (Fig. 1, heavy solid line) is not crossed. The x dependence of the isomer-shift data at low temperatures, however, shows a first-order jump. The $x = 0.175$ sample contains both ~ 2.8 -valent and ~ 2.2 -valent Eu. This coexistence of two types of Eu can again be traced to the aforementioned spatial inhomogeneities.

The ~ 2.8 -valent phase exhibits enhanced Pauli paramagnetism down to 1.2 K, typical of mixed-valent materials. On the other hand the magnetically split Mössbauer spectra of the $x = 0.20$ and $x = 0.25$ samples in this system unambiguously establish the onset of a magnetically ordered ground state in this concentration range. The magnetic susceptibility data (Fig. 2) imply some antiferromagnetic-type spin arrangement. From the collapse of the spontaneous hyperfine field as observed by the Mössbauer effect and from the peak in the magnetic susceptibility we estimate the magnetic ordering temperatures to be $T_M = 32 \pm 1$ K ($x = 0.20$) and $T_M = 28 \pm 1$ K ($x = 0.25$). It should be noted that the valence of the $x = 0.25$ sample has been established as 2.18 ± 0.05 via L_{III} absorption spectroscopy, confirming the weakly mixed-valent character of this magnetically ordered compound.¹⁷

The magnetically split spectra were fitted by a superposition of Lorentzians typical of Eu.¹⁸ Excellent fits were obtained only after a Lorentzian distribution of internal hyperfine fields was included in the fitting procedure. This hyperfine-field distribution is consistent with the concentration gradient mentioned above. The thermal variation of the spontaneous internal hyperfine field for the $x = 0.25$ sample is well described by a $J = \frac{7}{2}$ Brillouin function, with an ordering temperature $T_N = 27.7$ K and a saturation field $H_{hf}(0) = 450$ kG (Fig. 4). The hyperfine field at 11 K for the magnetically ordered regions of the $x = 0.175$ sample was 455 ± 3 kG implying an increase in saturation hyperfine field with decreasing x in this range. This increase of $H_{hf}(0)$ coupled with the enhancement of T_N with decreasing x indicates that intersite magnetic exchange is strengthening while the magnetic moments remain stable as the valence transition is approached. Work on many

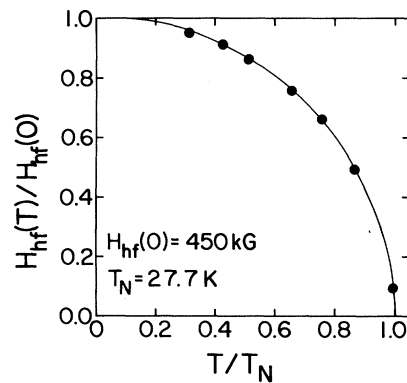


FIG. 4. The spontaneous hyperfine field, H_{hf} (circles), vs temperature in the antiferromagnetic phase of an $\text{Eu}(\text{Pd}_{1-x}\text{Au}_x)_2\text{Si}_2$ $x = 0.25$ sample. The error bars fall within the symbols. The solid line is the theoretical Brillouin function prediction for $J = \frac{7}{2}$.

Ce-based systems has indicated a similar magnetic-exchange enhancement but a contrasting magnetic-moment weakening, due to the Kondo effect, precursive to the Ce "valence" instability.^{4,19-20}

In the Eu system presented here, the two phase transitions are driven by intersite valence-fluctuation interactions and intersite magnetic (Ruderman-Kittel-Kasuya-Yosida) interactions. In this particular system the valence fluctuation interactions are dominant, causing a first order valence transition to abruptly terminate the magnetically ordered phase. The more interesting case where intersite magnetic interactions compete on an equal (or superior) footing with valence fluctuations should also be realizable, given the large number of Eu systems.

More generally, electronic transitions similar to the valence transition reported here are common in rare-earth materials. A few specific examples are pressure-induced transitions in SmS , EuO , Eu , Ce , CeP , CeAl_2 , and CeS .¹⁻⁴ In all of these materials one of the stable phases is known to be magnetic; however, in no system besides the one presented in this paper has the low-temperature region of the phase diagram, where magnetic order confronts the valence instability, been explored. Hopefully, the "blueprint" provided by the $\text{Eu}(\text{Pd}_{1-x}\text{Au}_x)_2\text{Si}_2$ phase diagram will focus experimental interest on the phase diagrams of these other systems. As more such phase diagrams emerge, the role of key parameters—such as magnetic state degeneracy, the Kondo effect, crystal structure, and conduction-band population—may be understood.

The authors would like to thank D. DiMarzio for assistance in fitting the internal-field variation by the Brillouin function. We also thank B. Grier and J. Hurst for communication of their x-ray diffraction data prior to publication.¹⁴ This work was supported in part by the Research Corporation, the U. S. Department of Energy under Grant No. DE-AS05-82ER12061, and the National Science Foundation under Grant No. DMR-8202726.

¹See *Valence Instabilities and Related Narrow Band Phenomena*, edited by R. D. Parks (Plenum, New York, 1977).

²See *Valence Fluctuations in Solids*, edited by L. Falicov, W. Hanke, and M. B. Maple (North-Holland, Amsterdam, 1981).

³See "Valence Instabilities," edited by J. Schoenes, J. Sierro, H. Ott, and P. Wachter (North-Holland, Amsterdam, to be published).

⁴J. M. Lawrence, P. S. Riseborough, and R. D. Parks, *Rep. Prog. Phys.* **44**, 1 (1981).

⁵J. Hansel, T. G. Philips, and G. A. Thomas, *Solid State Physics*, **32**, edited by H. Ehrenreich, F. Seitz, and D. Turnbull (Academic, New York, 1977), p. 88.

⁶D. B. McWhan, J. M. Rice, and J. P. Remeika, *Phys. Rev. Lett.* **23**, 1384 (1969); J. Wilson and G. D. Pitt, *Philos. Mag.* **23**, 1297 (1971).

⁷E. Sampathkumaran, L. C. Gupta, R. Vijayaraghavan, K. Gopalakrishnan, R. Pillay, and H. Devare, *J. Phys. C* **14**, L237 (1981).

⁸E. Sampathkumaran, R. Vijayaraghavan, K. Gopalakrishnan, R. Pillay, H. Devare, L. C. Gupta, B. Post, and R. D. Parks, *Ref. 2*, p. 193.

⁹L. C. Gupta, V. Murgai, Y. Yeshurun, and R. D. Parks, in *Ref. 3*.

¹⁰M. Croft, J. A. Hodges, E. Kemly, A. Krishnan, V. Murgai, and L. C. Gupta, *Phys. Rev. Lett.* **48**, 826 (1982).

¹¹I. Nowik, *Ref. 1*, p. 261; J. Coey and O. Massenet, *Ref. 1*, p. 211.

¹²E. Bauminger, D. Froindlich, I. Nowik, S. Ofer, I. Felner, and I. Mayer, *Phys. Rev. Lett.* **30**, 1053 (1973).

¹³J. Lawrence, M. Croft, and R. D. Parks, *Ref. 1*, p. 35.

¹⁴B. Grier and J. Hurst, private communication.

¹⁵W. Franz, A. Griessel, F. Steglich, and D. Wohlleben, *Z. Phys. B* **31**, 7 (1978).

¹⁶For a more complete description, see M. Croft, C. U. Segre, J. A. Hodges, A. Krishnan, V. Murgai, L. C. Gupta, and R. D. Parks, in *Ref. 3*.

¹⁷V. Murgai, L. C. Gupta, and R. D. Parks, to be published.

¹⁸*Mössbauer Spectroscopy*, edited by N. N. Greenwood and T. C. Gibb (Chapman and Hall, London, 1971), pp. 59-63, 543-555, 616.

¹⁹See, for example, M. Croft, R. P. Guertin, L. C. Kupferberg, and R. D. Parks, *Phys. Rev. B* **20**, 2073 (1979); H. H. Levine and M. Croft, *Ref. 2*, p. 279; M. Croft and H. H. Levine, *J. Appl. Phys.* **53**, 2122 (1982).

²⁰See, for example, J. M. Lawrence and M. T. Béal-Monod, *Ref. 2*, p. 53; J. M. Lawrence, *J. Appl. Phys.* **53**, 2117 (1982).

Investigation of the Ribbon Structure of a Lyotropic Liquid Crystal by Deuterium Nuclear Magnetic Resonance

G. Chidichimo,^(a) N. A. P. Vaz,^(b) Z. Yaniv, and J. W. Doane

Department of Physics and Liquid Crystal Institute, Kent State University, Kent, Ohio 44242

(Received 7 October 1982)

This paper reports observation, in a mixture of potassium palmitate- d_3 , potassium laurate, and water, of a lamellar phase above 41°C, a phase of elongated cylindrical aggregates below 36°C, and, in the intermediate temperature region, a phase in which the ²H-NMR spectral patterns can be calculated from a model of elongated ribbon-shaped aggregates. The size of the ribbons can be determined from the spectra and is found to vary with temperature. The results are consistent with ²H-NMR spectra of ²H₂O in the same and other ternary mixtures.

PACS numbers: 64.70.Ew, 61.30.Gd

Lyotropic phases intermediate in concentration or temperature between the lamellar and hexagonal phases (elongated cylindrical aggregates) have been of current interest.¹⁻³ Some of these studies have been stimulated by the recent discovery

of a biaxial lyotropic nematic found to exist in a short temperature interval between nematic phases of type I (elongated aggregates) and of type II (lamellar aggregates).⁴ One such study is that of Hendrikx and Charvolin,² who have examined the

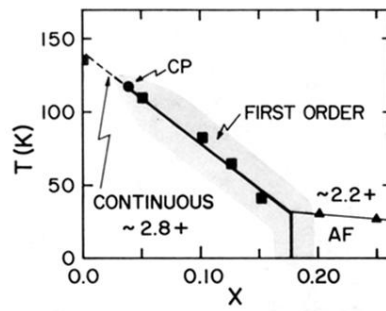


FIG. 1. Phase diagram for the $\text{Eu}(\text{Pd}_{1-x}\text{Au}_x)_2\text{Si}_2$ systems, discussed in the text. The shaded region indicates the inhomogeneity smearing of the valence transition in this and subsequent figures.

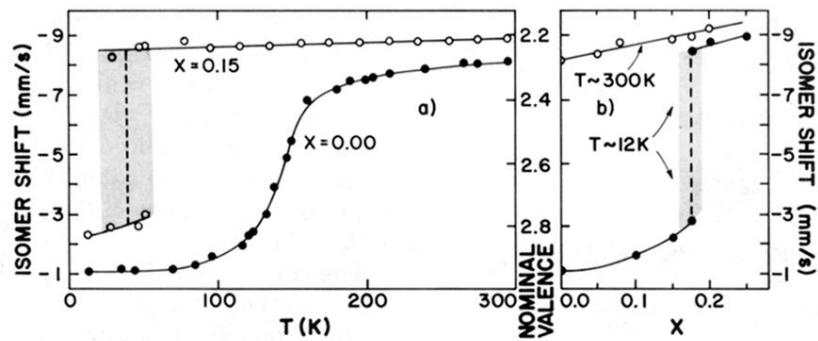


FIG. 3. (a) Thermal variation of the isomer shifts for an $x = 0.15$ sample (and for an $x = 0.00$ sample for comparison). The open circles are the isomer shifts of the $\text{Eu}^{2.2+}$ and $\text{Eu}^{2.8+}$ lines in the $x = 0.15$ sample. The solid lines are guides to the eye, the dashed line indicates the valence transition temperature assigned as described in the text. (b) Isomer-shift variation as a function of x across the valence transition at $T \sim 12$ K and at $T \sim 300$ K where no valence transition occurs.